Edge-Coupled Terahertz Photomixer Sources for On-Chip Sensing Applications

Daryoosh Saeedkia, Mohammad Neshat, and Safieddin Safavi-Naeini
Electrical and Computer Engineering Department, University of Waterloo
Waterloo, Ontario, Canada N2L 3G1
Email: {daryoosh, mneshat, safavi}@maxwell.uwaterloo.ca

***Abstract*— The waveguiding properties of a multilayer dielectric slab waveguide structure with applications in edge-coupled terahertz photomixer sources are studied. The structure guides two interfering laser beams, which their central frequency difference falls into the terahertz spectrum. The top layer of the dielectric waveguide structure is made of an ultra-fast photoabsorbing material, wherein the power of the guided modes are being absorbed and converted into a terahertz signal. The optical field and power distributions inside the waveguide structure are studied for different physical parameters of the dielectric layers. The generated terahertz photocurrent and terahertz power inside the photoabsorbing layer are calculated.**

I. Introduction

Terahertz technology is a fast-growing field [1], [2] with applications in biology and medicine [3]-[5], medical imaging [6], material spectroscopy and sensing [7], security [8], monitoring and spectroscopy in pharmaceutical industry [9], and high-data-rate communications [10]. The direction of the terahertz technology is towards the implementation of compact and cost-efficient systems for different terahertz applications. Realization of a compact, high-power, and low-cost terahertz source is a crucial step towards this goal.

In the edge-coupled photomixer sources [11]-[15], the laser beams are guided inside an optical dielectric waveguide structure and being absorbed by an overlying ultra-fast photoabsorbing layer, wherein a terahertz signal is generated due to photomixing phenomena. The generated terahertz signal is guided by a transmission line, which can be a coplanar stripline (CPS), a coplanar waveguide (CPW), or a parallel-plate waveguide. The edge-coupled photomixer sources are attractive for system-on-chip configurations for terahertz spectroscopy and sensing and terahertz imaging applications.

To design and optimize an edge-coupled terahertz photomixer source, it is important to know the optical power distribution across the optical waveguide and also its variation along the waveguide. In this paper, we study the waveguiding properties of a multilayer dielectric slab waveguide structure with application in edge-coupled terahertz photomixer sources. We evaluate the modal field distribution for this structure and calculate the absorbed optical power and the generated terahertz photocurrent and terahertz power inside the ultra-fast photoabsorbing layer. The presented model can be used for designing and optimization of terahertz photomixer sources with guided-wave optical excitation scheme.

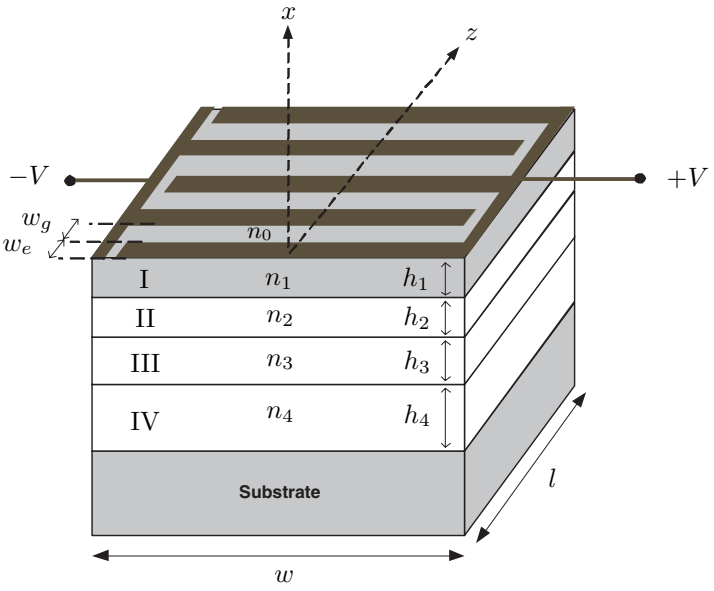

Fig. 1. Schematic of a five-layer dielectric slab waveguide for terahertz edge-coupled photomixer applications. Two frequency-detuned interfering laser beams uniformly shine the entire x-y facet of the five-layer waveguide structure and excite guided modes traveling along z-axis. Region I is made of an ultra-fast photoabsorbing layer, wherein the optical power is being absorbed and converted into a terahertz signal.

II. Multilayer Dielectric Slab Waveguide

Fig. 1 shows a five-layer optical waveguide structure with $n_1 > n_3 > n_2 = n_4$, where layer I is made of an ultra-fast photoabsorbing material, such as low-temperature grown (LTG) GaAs [16] or ErAs:$In_{0.53}Ga_{0.47}As$ [17], [18], and regions II, III, and IV are epitaxially grown over an appropriate substrate and are transparent at the operating optical wavelengths. Two practical material systems for edge-coupled terahertz photomixers are $Al_{\xi}Ga_{1-\xi}As$ [12], [14] for the wavelengths around 780 nm and $In_{1-x}Ga_xAs_yP_{1-y}$ [13], [19] for the wavelengths around 1550 nm. In the edge-coupled photomixer structure shown in Fig. 1, two frequency-detuned interfering laser beams uniformly shine the entire facet of the five-layer dielectric waveguide structure in x-y plane. If the effective refractive index of a guided mode, $n_e = \beta/k_0$, is in the range of $n_3 < n_e < n_1$, the corresponding mode is in the form of a guided field inside region I and an evanescent field inside region III. If n_e is in the range of $n_2 < n_e < n_3$,

the corresponding mode is in the form of guided fields inside both regions I and III. Satisfying the following conditions together guarantees the single-mode operation of the five-layer dielectric waveguide [20]

$$h_1 \leq \frac{\lambda \tan^{-1}\left(\sqrt{\frac{n_3^2-n_0^2}{n_1^2-n_2^2}}\right)}{2\pi\sqrt{n_1^2-n_2^2}} \quad (1)$$

$$h_3 \leq \frac{\lambda}{2\sqrt{n_3^2-n_2^2}} \quad (2)$$

$$h_2 > \lambda \quad (3)$$

Fig. 2 shows the amplitude of the electric field distribution across the five-layer waveguide structure at $z = 0$. The waveguide consists of $In_{0.75}Ga_{0.25}As_{0.54}P_{0.46}$ with the refractive indices $n_2 = n_4 = 3.36$ (at $\lambda = 1550$ nm) as regions II and IV, $In_{0.7}Ga_{0.3}As_{0.64}P_{0.36}$ with the refractive index $n_3 = 3.40$ as region III, and ErAs:$In_{0.53}Ga_{0.47}As$ with the refractive index $n_1 = 3.54$ as region I.

From (1)-(3), the conditions for having only one guided mode inside the five-layer waveguide structure are $h_1 \leq 0.274$ μm, $h_3 \leq 1.49$ μm and $h_2 > 1.55$ μm. For the cases shown in Fig. 2, the thicknesses of the dielectric layers satisfy the single-mode operation conditions. For all the cases, the effective refractive indices are smaller than n_3, which results in guided fields inside both region I and region III. As it can be seen from Figs. 2(a) and 2(b), one can control the amount of the coupled optical power into the photoabsorbing layer by changing either the thickness of the photoabsorbing layer or the thickness of the region III.

Fig. 3 shows the amplitude of the electric field distribution across a five-layer dielectric waveguide, where both waveguide I and waveguide III are strongly guiding waveguides. For this structure, the region I is made of ErAs:$In_{0.53}Ga_{0.47}As$ with the refractive index $n_1 = 3.54$, the regions II and IV are made of $In_{0.79}Ga_{0.21}As_{0.45}P_{0.55}$ with the refractive indices $n_2 = n_4 = 3.3$, and the region III is made of $In_{0.65}Ga_{0.35}As_{0.75}P_{0.25}$ with the refractive index $n_3 = 3.44$. The single mode operation conditions for this structure from (1)-(3) are $h_1 \leq 0.248$ μm, $h_3 \leq 0.898$ μm and $h_2 > 1.55$ μm. As it can be seen from Fig. 3, for large h_3, the optical power is strongly confined inside the region III. In order to have a reasonable optical power coupled to the photoabsorbing layer, the thickness of the region III must be small.

For an optimum edge-coupled photomixer design the coupled optical power to the photoabsorbing layer should be as high as possible below the device's burnout condition.

Fig. 4 shows the total optical intensity distribution across the five-layer dielectric waveguide at different points along the waveguide. As the optical signal propagates along the waveguide, its power is being gradually absorbed by the photoabsorbing layer.

Fig. 5 shows the total optical power inside the photoabsorbing layer along the z-axis for different values of the thicknesses of the dielectric layers. The total input optical power is

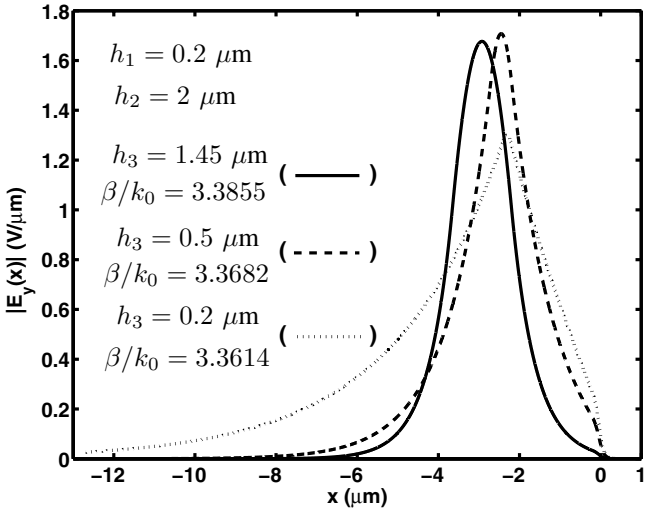

(a)

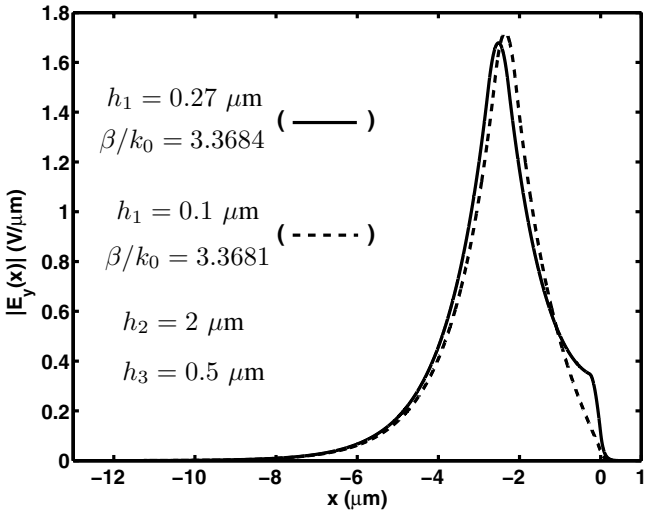

(b)

Fig. 2. Amplitude of the electric field distribution across the five-layer dielectric waveguide structure at $z = 0$. The refractive indices of the layers are $n_0 = 1$, $n_1 = 3.54$, $n_2 = n_4 = 3.36$, and $n_3 = 3.40$, (a) $h_1 = 0.2$ μm, $h_2 = 2$ μm, $h_3 = 1.45$ μm (soild line), 0.5 μm (dashed line), 0.2 μm (dotted line), and $h_4 = 10.5$ μm (b) $h_1 = 0.27$ μm (soild line), 0.1 μm (dashed line), $h_2 = 2$ μm, $h_3 = 0.5$ μm, and $h_4 = 10.5$ μm. The optical wavelength is $\lambda = 1550$ nm.

200 mW. The total optical power inside the photoabsorbing layer decreases exponentially along the waveguide. The optical power decays faster for the cases where the amplitude of the electric field inside the photoabsorbing layer is larger. Since at each point along the waveguide only a portion of the optical power is coupled into the photoabsorbing layer, the optical power absorption rate inside the waveguide is smaller than the absorption rate in a bulk photoabsorbing material. This property allows one to inject higher optical power into the device and generate more terahertz power without burning out the device.

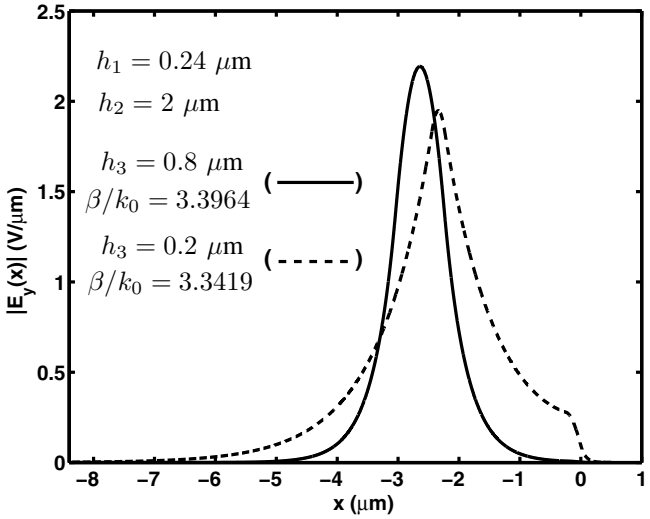

Fig. 3. Amplitude of the electric field distribution across the five-layer dielectric waveguide structure at $z = 0$. The refractive indices of the layers are $n_0 = 1$, $n_1 = 3.54$, $n_2 = n_4 = 3.33$, and $n_3 = 3.44$. The thicknesses of the dielectric layers are $h_1 = 0.24$ μm, $h_2 = 2$ μm, $h_3 = 0.8$ μm (soild line), 0.2 μm (dashed line), and $h_4 = 5$ μm. The optical wavelength is $\lambda = 1550$ nm.

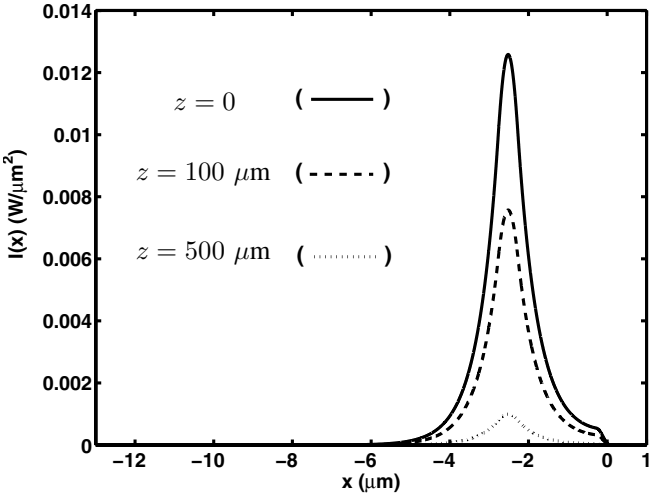

Fig. 4. Total optical intensity across the five-layer dielectric waveguide at different points along the waveguide. The refractive indices of the layers are $n_0 = 1$, $n_1 = 3.54$, $n_2 = n_4 = 3.36$, and $n_3 = 3.40$. The thicknesses of the dielectric layers are $h_1 = 0.27$ μm, $h_2 = 2$ μm, $h_3 = 0.5$ μm, and $h_4 = 10.5$ μm. The total optical power is 100 mW. The optical wavelength is $\lambda = 1550$ nm.

III. Terahertz Photocurrent and Power

Shown in Fig. 6 is the z-component of the generated terahertz photocurrent inside the photoabsorbing layer and at two different depths for a structure with parameters given in Table I. The thickness of the photoabsorbing layer is 200 nm, hence, the bias field distribution inside this layer is almost uniform. The generated photocurrent is higher at $x = -200$ nm, where the optical field is stronger (see Fig. 2a).

The generated terahertz power inside the photoabsorbing layer can be calculated as

$$P_{THz} = \frac{w}{T} \int_0^T \int_0^{h_1} \int_0^l \boldsymbol{\mathcal{E}}_{ind}(x,z;t) \cdot \boldsymbol{\mathcal{J}}_{THz}(x,z;t)\, dx\, dz dt \tag{4}$$

where $T = 2\pi/\Omega$ is the temporal period of the generated terahertz signal, $\boldsymbol{\mathcal{E}}_{ind}(x,z;t)$ is the induced time varying electric field inside the photoabsorbing layer due to carrier separation mechanism and due to the creation of excess charge density resulting from unequal electron and hole recombination lifetimes [21], and $\boldsymbol{\mathcal{J}}_{THz}(x,z;t)$ is the terahertz photocurrent.

The generated terahertz power for a structure with parameters given in Table I and with $h_1 = 200$ nm, $h_2 = 2$ μm, $h_3 = 200$ nm, and $h_4 = 10.5$ μm is 1 μW at 1 THz beat frequency for the total optical power of 400 mW. This power level is sufficient for on-chip terahertz sensing and spectroscopy applications.

IV. Conclusion

A multilayer dielectric slab waveguide structure with an ultra-fast photoabsorbing top layer has been studied for the applications in edge-coupled terahertz photomixer sources. The modal analysis of a five-layer dielectric waveguide has been presented and the optical field and power distributions across the waveguide for different physical parameters of the dielectric layers have been studied. Also, the optical power coupling into the photoabsorbing layer has been studied in detail. The generated terahertz photocurrent and terahertz power inside the photoabsorbing layer are calculated. The proposed model can be used for designing and optimization of the edge-coupled terahertz photomixer sources.

TABLE I

Physical and dimensional parameters of a designed photomixer

Description	Notation	Value
Laser central wavelength	λ_1	1550 nm
Applied dc voltage	V	10 V
Each laser power	P_{opt}	100 mW
Optical absorption coefficient[18]	α	7500 cm^{-1}
Carrier saturation velocity[18]	v_{sat}	60 m/ms
Carrier lifetime[17]	τ	0.5 ps
Electron (hole) mobility[22]	μ_n (μ_p)	1700 (68) cm^2/Vs
Device width	w	6 μm
Electrode width	w_e	2 μm
Gap between electrode fingers	w_g	2 μm
Core refractive index	n_1 (n_3)	3.54 (3.40)
Cladding refractive index	n_2, n_4	3.36
Electrode refractive index @ 1550 nm	n_0	$0.4790 - j10.806$

Acknowledgment

This research is funded by the NSERC/RIM Industrial Research Chair Program and by Ontario Centres of Excellence (OCE).

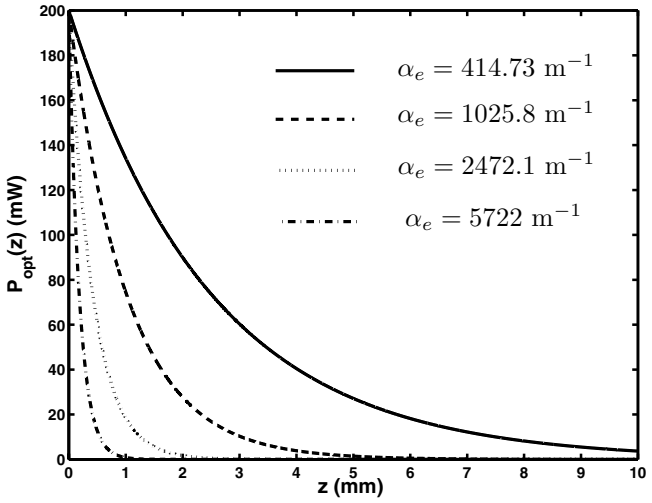

Fig. 5. Total optical power inside the five-layer dielectric waveguide along the z-axis for different values of the thicknesses of the dielectric layers: $(h_1, h_2, h_3) = (0.2, 2, 0.5)$ μm (solid-line), $(h_1, h_2, h_3) = (0.2, 2, 0.2)$ μm (dashed line), $(h_1, h_2, h_3) = (0.27, 2, 0.5)$ μm (dotted line), $(h_1, h_2, h_3) = (0.2, 0.2, 1.7)$ μm (dash-dot line), $h_4 = 10.5$ μm. The refractive indices of the layers are $n_1 = 3.54$, $n_2 = n_4 = 3.36$, and $n_3 = 3.40$. The total optical power is 200 mW and the width of the waveguide is $w = 6$ μm. The optical wavelength is $\lambda = 1550$ nm.

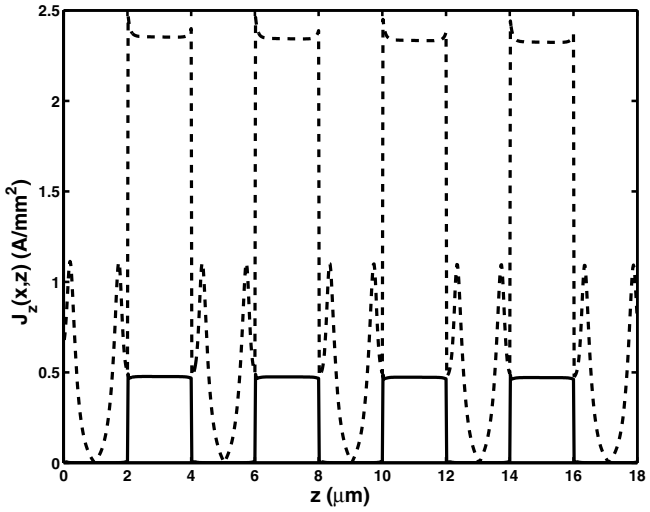

Fig. 6. Terahertz photocurrent along the waveguide at f= 1 THz and at two different depths: x=-20 nm (solid line) and x=-200 nm (dashed line). The thicknesses of the dielectric layers are: $h_1 = 200$ nm, $h_2 = 2$ μm, $h_3 = 200$ nm, and $h_4 = 10.5$ μm.

REFERENCES

[1] D. L. Woolard, E. R. Brown, M. Pepper, and M. Kemp, "Terahertz Frequency Sensing and Imaging: A Time of Reckoning Future Applications?" *Proceedings of the IEEE*, vol. 93, no. 10, pp. 1722–1743, 2005.

[2] K. Sakai, Ed., *Terahertz Optoelectronics*. Springer-Verlag, 2005.

[3] M. Nagel, P. Haring Bolivar, and H. Kurz, "Modular parallel-plate THz components for cost-efficient biosensing systems," *Semicond. Sci. Technol.*, vol. 20, no. 7, pp. S281–S285, 2005.

[4] P. H. Siegel, "Terahertz Technology in Biology and Medicine," *IEEE Trans. Microwave Theory Tech.*, vol. 52, no. 10, pp. 2438–2447, 2004.

[5] T. Globus, D. Woolard, M. Bykhovskaia, B. Gelmont, L. Werbos, and A. Samuels, "THz-frequency spectroscopic sensing of DNA and related biological materials," *International Journal of High Speed Electronics and Systems*, vol. 13, no. 4, pp. 903–936, 2003.

[6] S. Wang, B. Ferguson, D. Abbott, and X.-C. Zhang, "T-ray imaging and tomography," *J. Biol. Phys.*, vol. 29, no. 2-3, pp. 247–256, 2003.

[7] D. Mittleman, Ed., *Sensing with Terahertz Radiation*. Springer-Verlag, 2003.

[8] M. C. Kemp, P. F. Taday, B. E. Cole, J. A. Cluff, A. J. Fitzgerald, and W. R. Tribe, "Security applications of terahertz technology," in *The Proceedings of SPIE Conference*, vol. 5070, August 2003, pp. 44–52.

[9] P. F. Taday, "Applications of terahertz spectroscopy to pharmaceutical sciences," *Phil. Trans. R. Soc. Lond. A*, vol. 362, no. 1815, pp. 351–364, 2004.

[10] A. Hirata, H. Ishii, and T. Nagatsuma, "Design and characterization of a 120-GHz millimeter-wave antenna for integrated photonic transmitters," *The Proceedings of International Topical Meeting on Microwave/Photonics*, pp. 229–232, 2000.

[11] E. A. Michael, "Travelling-wave photonic mixers for increased continuous-wave power beyond 1 THz," *Semicond. Sci. Technol.*, vol. 20, no. 7, pp. S164–S177, 2005.

[12] J.-W. Shi, K.-G. Gan, Y.-J. Chiu,Y.-H. Chen, C.-K. Sun, Y.-J. Yang, and J. E. Bowers, "Metal-semiconductor-metal traveling-wave photodetectors," *IEEE Photon. Technol. Lett.*, vol. 16, no. 6, pp. 623–625, 2001.

[13] A. Stohr, R. Heinzelmann, A. Malcoci, and D. S. Jager, "Optical Heterodyne Millimeter-Wave Generation Using 1.55-μm Traveling-Wave Photodetectors," *IEEE Trans. Microwave Theory Tech.*, vol. 49, no. 10, pp. 1926–1933, 2001.

[14] L. Y. Lin, M. C. Wu, T. Itoh, T. A. Vang, R. E. Muller, D. L. Sivco, and A. Y. Cho, "High-Power High-Speed Photodetectors-Design, Analysis, and Experimental Demonstration," *IEEE Trans. Microwave Theory Tech.*, vol. 45, no. 8, pp. 1320–1331, 1997.

[15] E. H. Bottcher and D. Bimberg, "Millimeter wave distributed metal-semiconductor-metal photodetectors," *Appl. Phys. Lett.*, vol. 66, no. 26, pp. 3648–3650, 1995.

[16] G. L. Witt, R. Calawa, U. Mishra, and E. Weber, Eds., *Low Temperature (LT) GaAs and Related Materials*. Materials Research Society, 1992.

[17] E. R. Brown, D. C. Driscoll, and A. C. Gossard, "State-of-the-art in 1.55-μm ultrafast InGaAs photoconductors, and the use of signal-processing techniques to extract the photocarrier lifetime," *Semicond. Sci. Technol.*, vol. 20, no. 7, pp. S199–S204, 2005.

[18] M. Sukhotin, E. R. Brown, A. C. Gossard, D. C. Driscoll, M. Hanson, P. Maker, and R. Muller , "Photomixing and photoconductor measurements on ErAs/InGaAs at 1.55 μm," *Appl. Phys. Lett.*, vol. 82, no. 18, pp. 3116–3118, 2003.

[19] A. Stohr, A. Malcoci, A. Sauerwald, I. C. Mayorga, R. Gusten, and D. S. Jager, "Ultra-Wide-Band Traveling-Wave Photodetectors for Photonic Local Oscillators," *J. Lightwave Technol.*, vol. 21, no. 12, pp. 3062–3070, 2003.

[20] D. Saeedkia and S. Safavi-Naeini, "Modeling and Analysis of a Multilayer Dielectric Slab Waveguide With Applications in Edge-Coupled Terahertz Photomixer Sources," *J. Lightwave Technol.*, vol. 25, no. 1, pp. 432–439, 2007.

[21] ——, "A Comprehensive Model for Photomixing in Ultrafast Photoconductors," *IEEE Photon. Technol. Lett.*, vol. 18, no. 13, pp. 1457–1459, 2006.

[22] M. Sukhotin, E. R. Brown, D. C. Driscoll, M. Hanson, and A. C. Gossard, "Picosecond photocarrier-lifetime in ErAs:InGaAs at 1.55 μm," *Appl. Phys. Lett.*, vol. 83, no. 19, pp. 3921–3923, 2003.